JOURNAL OF SOLID STATE CHEMISTRY 94, 319–328 (1991)

Mechanistic Studies on the Electrochemically Lithiated Spinel $LiCuVO_4$

R. KANNO,* Y. TAKEDA,† M. HASEGAWA,†,‡ Y. KAWAMOTO, AND O. YAMAMOTO†

Department of Chemistry, Faculty of Science, Kobe University, Kobe, 657 Japan; and †Department of Chemistry, Faculty of Engineering, Mie University, Tsu, 514 Japan

Received November 19, 1990; in revised form June 3, 1991

The lithiation mechanism of the spinel $LiCuVO_4$ was studied by X-ray diffraction, XPS, and electrochemical measurements using the lithium cell with the spinel cathode. The lithiation proceeded by the following steps: (1) in the multiphasic reaction for $x < 1.5$ in $Li_{1+x}CuVO_4$, the $LiCuVO_4$ spinel transforms to a new phase, $Li_{2.5}Cu_{0.5}VO_4$, and Cu metal; (2) in the monophasic electrochemical displacement reaction for $1.5 < x < 2.0$, the copper ions extrude from $Li_{2.5}Cu_{0.5}VO_4$ with lithium intercalation, which forms Li_3VO_4 and Cu metal; (3) in the intercalation reaction for $2.0 < x < 5.0$, lithium ions intercalate into Li_3VO_4 with several reaction steps. The new phase, $Li_{2.5}Cu_{0.5}VO_4$, lithiated reversibly with the electrochemical displacement between copper and lithium ions.

Introduction

A wide variety of metal oxides and chalcogenides with two-dimensional layer structures or three-dimensional framework tunnel structures have been studied as the cathode material for secondary organic electrolyte lithium batteries (*1*). Most previous studies have focused on two-dimensional metal chalcogenides such as TiS_2, although metal oxides with framework structure such as V_6O_{13}, Cr_3O_8 and a number of MO_2 oxides with the rutile structure have demonstrated reversible lithium incorporation with high lithium ionic diffusion (*2–4*).

The spinel structure was recently found to be one of the framework structures suitable for lithium ionic diffusion; spinel compounds have thus been investigated not only as mixed conductors but also as pure ionic conductors (*5, 6*). The oxide and sulfide spinels were previously studied as possible solid-solution electrodes and their electrochemical performance and lithium-intercalated structures have been investigated for Fe_3O_4, Mn_3O_4, and a family of LiM_2O_4 compounds (M = Ti, V, Mn) (*7–11*). However, studies on lithium insertion into the oxide spinels suggested that lithium diffusion is too slow for these materials to be used as high-drain secondary battery cathodes. The bottleneck size of the oxide spinels is too small for high lithium ionic diffusion, or the diffusion in the princi-

* To whom correspondence should be addressed.

‡ Present address: Living Systems Research Center, Matsushita Electric Industrial Co., LTD, Moriguchi, Osaka 570, Japan.

0022-4596/91 $3.00

pal pathway is blocked by an immobile cation (*12*). If there are larger bottleneck sizes and no blocking ions on the A sites of the spinels, fast ionic conduction is observed: the defect inverse spinel $Li_{0.8}[Li_{0.8}Mg_{1.2}]Cl_4$ has a high ionic conductivity of $\sigma_{Li} = 5 \times 10^{-5}$ S cm^{-1} at 293 K (*13*).

The blocking effects on the diffusion pathway could be avoided in a structure containing either a cation that is mobile during the lithiation process or vacancies situated along the diffusion pathway. We reported that the copper ions in the ternary Chevrel phase $Cu_xMo_6S_8$ can be displaced electrochemically by lithium ions (*14*). After being discharged, the $Li/Cu_xMo_6S_8$ cells are fully converted to pure Li/Mo_6S_8 cells. A high diffusion rate of copper ions in the Chevrel structure makes it easier to displace copper ions by lithium ions in the Mo_6S_8 framework structure. The electrochemical displacement reaction might thus be expected for the spinel containing copper ions which are one of the best mobile species in the framework structure.

We recently reported the structure of the copper vanadate spinel $Li_{1+x}CuVO_4$ with one-dimensional cooperative ordering of the Jahn–Teller ion (*15*). In the orthorhombic structure with cell constants $a = 5.651$ Å, $b = 5.798$ Å, and $c = 8.747$ Å, the vanadium ions are tetrahedrally surrounded by oxide ions and the copper and lithium ions are distributed over the octahedral sites in an ordered manner. In the present study, we found that the copper vanadate spinel $LiCuVO_4$ was able to be lithiated reversibly and $LiCuVO_4$ is a cathode candidate for secondary lithium batteries. Further, the lithiation mechanism was examined by X-ray diffraction (XRD), XPS, and electrochemical measurements; details of the performance of the $Li/LiCuVO_4$ spinel cells are also presented.

Experimental

Samples were prepared by heating a mixture of CuO, V_2O_5, and Li_2CO_3 at 530°C in air. The reaction products were identified by the XRD method (Rigaku 12 kW) using monochromated Cu$K\alpha$ and a scintillation detector. The lithiated samples were protected by a 7-μm thick aluminum window which covered the sample holder to prevent moisture attack during the measurement. The lattice parameters were calculated using silicon as an internal standard. The cells used for electrochemical tests were constructed in a cylindrical configuration. The anode was a disk of lithium foil 14 mm in diameter and 0.24 mm in thickness. The separator was a microporous polypropylene sheet. The cathode comprised a mixture of 0.05 g of the oxides, 0.01 g acetylene black, and 0.001 g Teflon powder, which was pressed into a tablet 13 mm in diameter. The electrolyte was 1 *M* $LiClO_4$ in a 1 : 1 mixture of propylene carbonate and 1,2-dimethoxyethane by weight. The water content of the electrolyte was less than 20 ppm. The electrochemical measurements were carried out at room temperature after an overnight stand under zero current flow. Cell properties were measured galvanostatically, Quasi-open-circuit voltages (OCV) were measured by alternating discharge (200 μA, 3 hr) and rest (3 hr) periods.

Results and Discussion

Discharge Characteristics of $LiCuVO_4$

The electrochemical reaction of the spinel $LiCuVO_4$ with lithium is presented in Fig. 1, where the OCV of the cell is plotted as a function of the number of reacting lithium atoms, x. The copper vanadate spinel showed high working voltage and relatively large specific capacity. Table I shows discharge performances of $LiCuVO_4$ together with the spinel cathodes reported previously. The copper vanadate spinel showed a larger extent of lithium insertion than the other spinels, and also showed higher cell voltage ($V \simeq 2$ V) than the sulfide spinel ($V \simeq 1.5$ V). The energy density of the copper vanadate is much higher than that of the

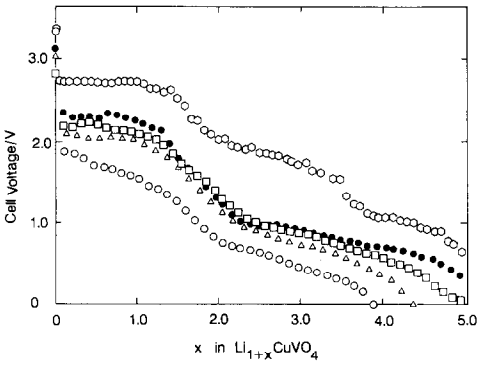

FIG. 1. The constant discharge curves of the cell, $Li/LiCuVO_4$, together with the OCV curve; ⬡. The discharge currents are as follows: ●, 0.2 mA/cm²; □, 0.5 mA/cm²; △, 1.0 mA/cm²; ○, 5.0 mA/cm².

sulfide spinel. Moreover, the copper vanadate spinel is rechargeable as discussed later.

Discharge Mechanism

Electrochemical characteristics of Li $CuVO_4$. The lithiation of $LiCuVO_4$ proceeded by several steps involving single-phase and multiphase electrode processes; they are characterized in the OCV curve shown in Fig. 1 by regions of decreasing voltage and of constant voltage, respectively. The OCV curve shows a potential plateau around 2.6 V for a composition of $0 < x < 1.5$ in $Li_{1+x}CuVO_4$, and after that a gently falling slope from $x = 2.0$ to 5.0 with a voltage knee around $x \simeq 3.5$ and 4.0. Multiphasic reaction indicated by the plateau of $0 < x < 1.5$ suggests the existence of a new phase at a composition of $x \simeq 1.5$. For $x > 1.5$, a gently falling slope in four steps indicates the homogeneous single phase formation at the composition ranges $1.5 < x \lesssim 2.0$, $\sim 2.0 < x \lesssim 3.5$, $\sim 3.5 < x \lesssim 4.0$, $\sim 4.0 < x < 5.0$.

XRD measurement. Figure 2 shows the variation of XRD patterns as a function of x in $Li_{1+x}CuVO_4$. The XRD patterns at $0 \leq x < 1.5$ showed the diffraction lines due to the spinel $LiCuVO_4$ together with broad extra lines, which are attributed to the new phase ($2\theta = 18.3°$, 23.1°, 28.4°, etc.) and copper metal ($2\theta = 28.5°$, 50.51°, etc.). The new phase exists at $x = 1.5$ ($Li_{2.5}Cu_{0.5}VO_4$), where the reflections due to $LiCuVO_4$ disappeared. No lattice parameter changes were observed for the orthorhombic cell in the composition range of $0 \leq x < 1.5$, indicating that the lithium ions did not intercalate into the spinel $LiCuVO_4$. Table II shows the XRD data of the new phase $Li_{2.5}Cu_{0.5}VO_4$. The XRD peaks in $Li_{2.5}Cu_{0.5}VO_4$ could be derived from the spinel; the peaks for example at $d = 4.822$ and 2.092 Å correspond respectively to those observed for the orthorhombic $(011)_o$ and $(101)_o$ peaks in $LiCuVO_4$ (derived from the $(111)_o$ reflection in the parent cubic cell), and the $(004)_o$ and $(220)_o$ peaks (derived from the $(400)_o$ reflection). The structure of $Li_{2.5}Cu_{0.5}VO_4$ is therefore basically composed of the cubic close anion packing similar to that of the spinel structure.

XPS measurement. The XPS and the Auger spectra were measured for the copper $2p$ 3/2 state, the vanadium $2p$ 3/2 state and the Cu_{LMN} at various lithiation levels. Figure 3 shows the Auger spectra of Cu_{LMN} of $Li_{1+x}CuVO_4$. At $x = 0$, the chemical shift of the Cu_{LMN} peak ($E = 336$ eV) is close to that of CuO (336.5 eV), indicating the divalent copper valence state in $LiCuVO_4$. At $x = 1.0$, the broad spectra near 335–338 eV showed a mixed valency with the chemical shifts of Cu^{+}_{LMN} in Cu_2O (338.1 eV), Cu^{2+}_{LMN} in CuO (336.5 eV), and Cu^{0}_{LMN} in Cu metal (335.6 eV) (20). For $x > 2.0$, the chemical shifts of Cu_{LMN} near 335 eV correspond to the metallic copper state. The XPS spectra of the vanadium $2p$ 3/2 state at $x = 0.0$, 1.0, and 2.0 in $Li_{1+x}CuVO_4$ showed the peak near $E = 517$ eV, which corresponds to that of V^{5+} $2p$ 3/2 in V_2O_5 (516.8 eV) (*21*). The peak shifts to lower binding energy with increasing lithiation from $x = 2.0$ to 4.0. At $x = 3.0$, a chemical shift of 516 eV corresponds to that of V^{4+} $2p$ 3/2 in VO_2 ($E = 515.7$ eV) (*21*).

TABLE Ia

DISCHARGE PERFORMANCE OF $LiCuVO_4$

Compound	Cutoff voltage (V)	Current density (mA/cm^2)	Mean discharge voltage (V)	Specific capacity (A hr/kg)	Energy density (W hr/kg)
$LiCuVO_4$	1.2	0.5	2.0	330	660
This work		1.0	1.9	290	545
	2.0	0.5	2.2	190	415
		1.0	2.2	150	330
		(OCV)	2.6	300	765
$CuCo_2S_4$ spinel, Ref. (*16*)	1.2	0.66	1.9	311	

Discharge mechanism. Given the electrochemical information and XRD and XPS data, we postulate the lithiation mechanism of $LiCuVO_4$ as follows:

(1) $x < 1.5$ ($x = a$)

$$LiCuVO_4 + a\,Li^+ + a\,e^- \rightarrow (1 - a/1.5)\,LiCuVO_4 + (a/1.5)\,Li_{2.5}Cu_{0.5}VO_4 + (1/2)(a/1.5)\,Cu,$$

(2) $1.5 < x < 2.0$ ($b = x - 1.5$)

$$Li_{2.5}Cu_{0.5}VO_4 + b\,Li^+ + b\,e^- \rightarrow Li_{2.5+b}Cu_{0.5-b}VO_4 + b\,Cu,$$

(3) $2.0 < x < 5.0$ ($c = x - 2.0$)

$$Li_3VO_4 + c\,Li^+ + c\,e^- \rightarrow Li_{3+c}VO_4,$$

At $x < 1.5$, the multiphase electrode process and the existence of the new phase at $x = 1.5$ are indicated by (i) the flat V_{OCV} versus x curve shown in Fig. 1, (ii) the disappearance of the spinel reflections at $x = 1.5$

TABLE Ib

OCV VOLTAGE AND CHARGE TRANSFER RANGE OF OXIDE SPINELS

Compound	Ref.	Range of x	Voltage (V)
$Li_xFe_3O_4$	*7*	0–3.0	3.1–1.2
$Li_{1+x}Fe_5O_8$	*17*	0–2.6	3–1.1
$Li_xFe_2O_3$	*7*	3–1.2	0–2.5
$Li_{1+x}Mn_2O_4$	*18*	0–0.9	3
		1.2–1.6	1.2
$Li_{1-x}Mn_2O_4$	*19*	0.9–0.6	3.2
$Li_xMn_3O_4$	*18*	0–0.8	3
		0.8–1.6	1.2
$Li_{0.94+x}VO_4$	*10*	0–0.45	2.4
		0.5–1.1	2.4–1.6
		1.1–1.2	1.6
$Li_{1+x}CuVO_4$	this work	0–1.5	2.8
		1.5–2.0	2.8–2.0
		2.0–3.5	2.0–1.5
		3.5–4.5	1.5–1.0

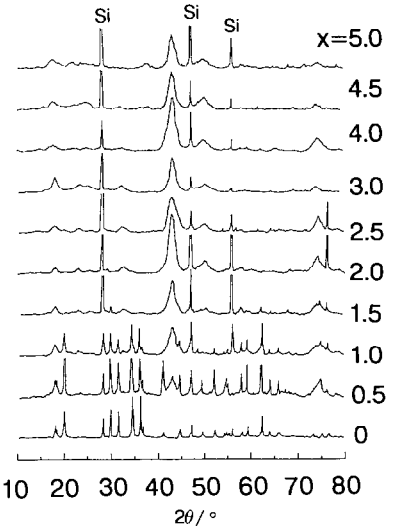

FIG. 2. X-ray diffraction patterns of $Li_{1+x}CuVO_4$ as a function of lithiation depth, x.

in the XRD data, and (iii) the mixed valence states of Cu^{2+}, Cu^{+}, and Cu^{0} at $x = 1.0$ in the XPS data. The composition of the new phase is therefore $Li^{I}_{2.5}Cu^{I}_{0.5}V^{V}O_4$. In the first lithiation process, copper metal deposits by the lithiation.

In the second step, monophasic reaction from $x = 1.5$ to 2.0 is indicated by the OCV measurement. The valence states Cu^{0} and V^{5+} at $x = 2.0$ observed in the XPS showed an extrusion of metallic copper; lithium ions inserted into, and copper ions extruded from the phase $Li_{2.5}Cu_{0.5}VO_4$.

The reaction at $x > 2.0$ was characterized by a continuous insertion of lithium into the phase "Li_3VO_4." However, the OCV curve shows a distinct voltage change near $x = 3.5$ and 4.0. This indicates a change in the lithiation process and the two-phasic reaction with narrow composition ranges near $x \simeq 3.5$ and 4.0. Further, the lithium insertion proceeded up to $x = 5.0$ (Li_6VO_4), where the vanadium ions must be divalent.

TABLE II

X-RAY POWDER DIFFRACTION DATA FOR $Li_{2.5}Cu_{0.5}VO_4$

d_{obs}	I_{obs}
4.822	w
3.811	vw
2.736	w
2.092	s
2.070	m
1.829	w
1.274	w

Cycling Characteristics of $LiCuVO_4$

The reversibility of the lithium/$LiCuVO_4$ cells was examined for the charge transfer ranges of $0 \leq x \leq 1.0$, $1.0 \leq x \leq 2.0$, and $2.0 \leq x \leq 3.0$ in $Li_{1+x}CuVO_4$, at a current density of 0.5 mA/cm^2. The

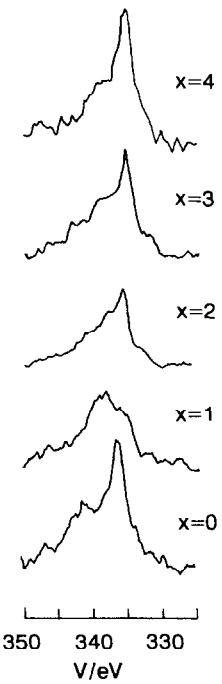

FIG. 3. Cu_{LMN} Auger spectra of $Li_{1+x}CuVO_4$ at various depths of discharge.

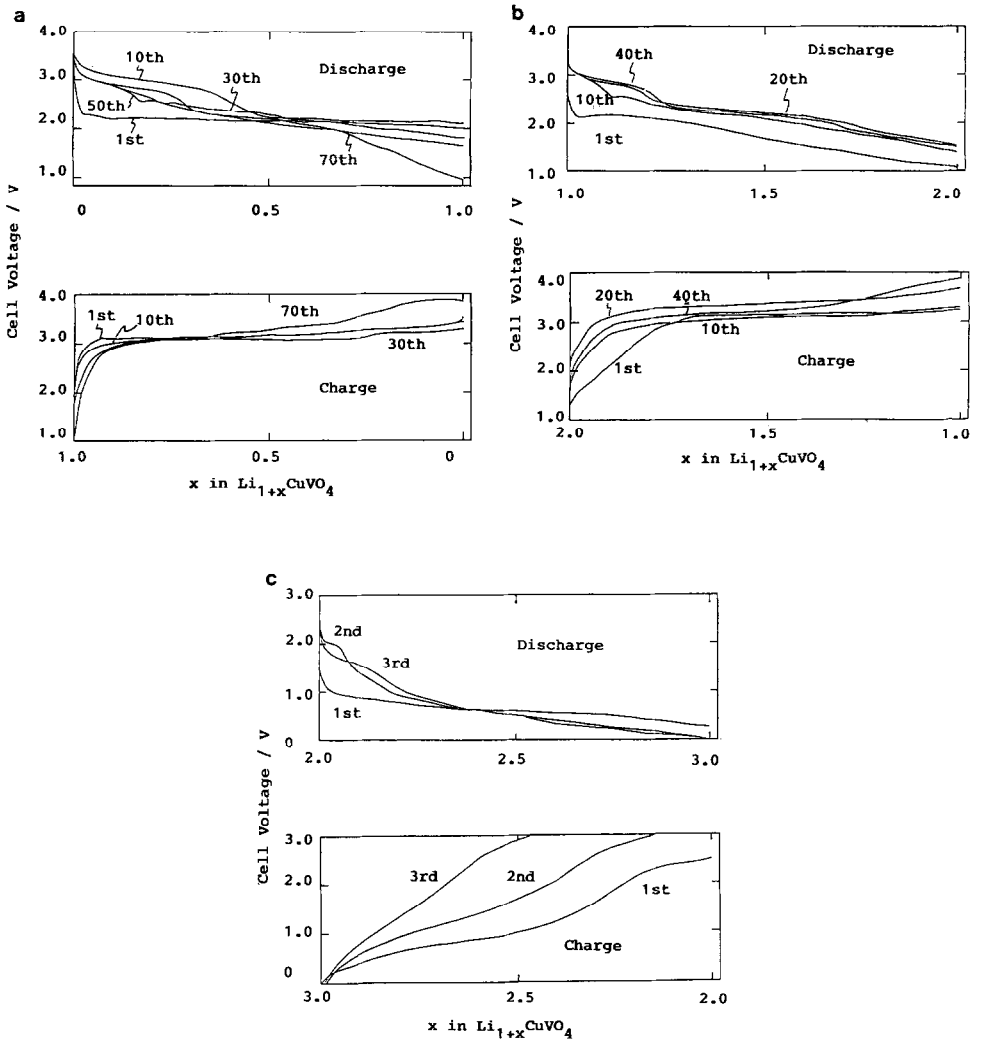

FIG. 4. Charge–discharge curves of the $Li/Li_{1+x}CuVO_4$ cell at a range of (a) $0 \leq x \leq 1.0$, (b) $1.0 \geq x \geq 2.0$, (c) $2.0 \geq x \geq 3.0$.

charge–discharge curves are shown in Fig. 4. For $0.0 \leq x \leq 1.0$, the charging efficiency of the first cycle was 100%. The cell voltage of $0 < x < 0.4$ on discharge increases with cycling up to 10th cycles; however, no significant degradation is found for the profile or efficiency after 10 cycles. For $0 \leq x \leq 2.0$, the efficiency of the first charge is also 100%. The cell voltages after 10 cycles are higher than those at the first cycle, and afterward no significant degradation in the profile is observed. The average cell voltage on the discharge is about 2.0 V, which is lower than that obtained for $0.0 \leq x \leq 1.0$. For $2.0 \leq x \leq 3.0$, the charging efficiency decreases with cycling and the average discharge voltage is less than 1.0 V.

Charge–Discharge Mechanism

The $Li/LiCuVO_4$ couple showed good reversibility in cell reaction for the charge transfer ranges of $0.0 \leq x \leq 1.0$ and $1.0 \leq$

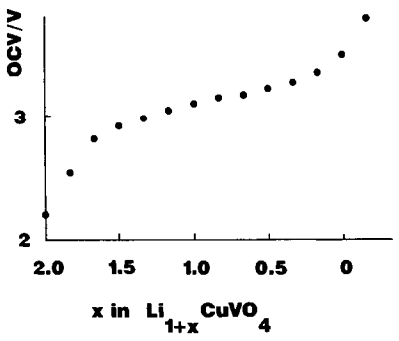

FIG. 5. Quasi-OCV curve of the cell, $Li/Li_{1+x}CuVO_4$, recharged from $x = 2.0$ to 0.0.

$x \leq 2.0$. However, the gradual change in the charge–discharge profile shown in Fig. 4 suggests the reaction mechanism change. The mechanism was therefore examined in order to clarify the good rechargeability of the lithium/$LiCuVO_4$ cell.

Electrochemical characteristics. Figure 5 shows the OCV curve of the cell recharged from $x = 2.0$ to 0.0 in $Li_{1+x}CuVO_4$. The cathodes discharged to $x = 2.0$ were recharged completely to the initial composition of $x = 0.0$. The OCV measurement proceeded below a decomposition voltage of the electrolyte. It is apparent from the gently falling OCV curve that the reaction proceeded by the monophasic electrode process in two steps: from $x = 2.0$ to 1.5 and from $x = 1.5$ to 0.0. The reaction was characterized by a continuous extrusion of lithium from "Li_3VO_4" at $x = 2.0$ to a composition of "$LiCuVO_4$" at $x = 0.0$. The XPS data at 2.0 showed a V^{5+} valence state, which indicates that the vanadium ions do not participate in the recharge reaction from $x = 2.0$ to 0.0. The copper metal extruded from the cathode therefore inserted again, satisfying the two-electron transfer for the recharge process.

XRD measurement. Figure 6 shows the XRD patterns of the sample charged from $x = 2.0$ to 0.0. No significant difference is found, except the peaks due to copper metal ($2\theta = 50.51°$ and 74.21°) disappeared. The lithium ions intercalated into the new phase were displaced electrochemically by copper ions.

Cycling characteristics of short charge transfer ranges. The cycling behavior was examined at different charge transfer levels with a shallow charge–discharge depth of 0.1 in $Li/Li_{1+x}CuVO_4$, in order to clarify the details of the charge–discharge process. The current density was 0.5 mA/cm^2. Figure 7 shows the cycling characteristics near $x = 0.5$, 1.0, and 2.0.

In $0.54 \leq x \leq 0.64$, the charge–discharge profiles change gradually from the 1st to the 100th cycle, and the plateaus region on discharge disappears after 60 cycles. The discharge proceeds from the 200th to the 500th cycle between 3.5 and 2.0 V. The terminating voltage on discharge decreases from 2.0 V at 500 cycles to 1.5 V at 800 cycles. For charging, the cell voltage increases from 3.0 V at the 1st cycle to 3.5 V at the 40th cycle, and afterward no significant profile change is observed up to 1000 cycles.

In $0.9 \leq x \leq 1.0$, the charge–discharge profiles change gradually from the 1st to the 120th cycles, whereas after 120 cycles, no remarkable change is found. The terminating voltage decreases from 2 V at 300 cycles to 1.5 V at 600 cycles.

In $1.95 \leq x \leq 2.05$, the charge–discharge cycles proceed between 3.0 and 1.0 V. The

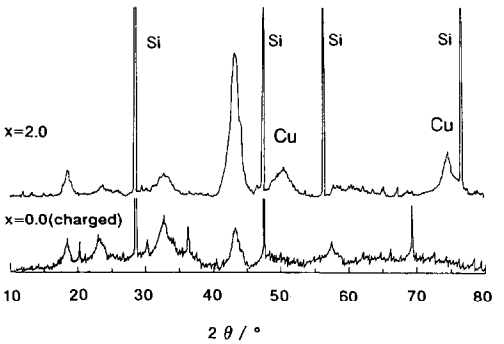

FIG. 6. X-ray diffraction patterns of $Li_{1+x}CuVO_4$ at $x = 2.0$ and 0.0. The pattern at $x = 0.0$ was measured after the sample was charged from $x = 2.0$.

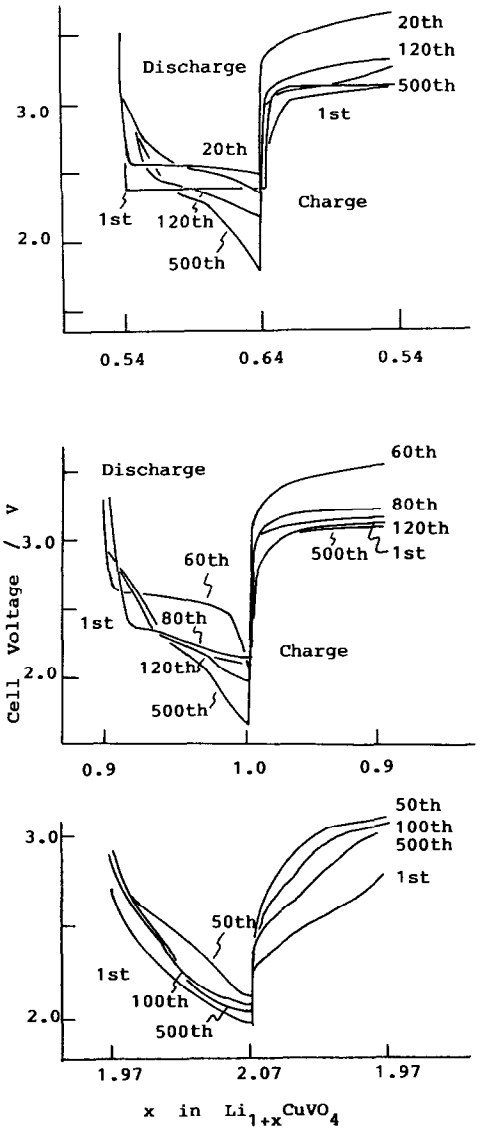

FIG. 7. Charge–discharge curves of the $Li/Li_{1+x}CuVO_4$ cell at a short charge transfer range of (a) $0.54 \leq x \leq 0.64$, (b) $0.95 \leq x \leq 1.0$, and (c) $1.95 \leq x \leq 2.05$.

profiles differ slightly from those for the $0.54 < x < 0.64$ and $0.9 < x < 1.0$ regions; however, no significant profile degradation is observed during cycling.

Charge–discharge mechanism of the Li/LiCuVO$_4$ cell. The OCV and XRD measurements of the samples recharged from $x = 2.0$ to 0.0 showed the reaction in two steps which were characterized by a continuous electrochemical displacement between lithium and copper ions. The charge reaction sequence could thus be represented as

(1) $2.0 > x > 1.5$, $a = 2.0 - x$

$$Li_{3.0}VO_4 + a\,Cu \rightarrow Li_{3-a}Cu_aVO_4 + a\,Li + a\,e^-$$

(2) $1.5 > x > 0.0$, $b = 1.5 - x$

$$Li_{2.5}Cu_{0.5}VO_4 + (1/3)\,b\,Cu \rightarrow Li_{2.5-b}Cu_{0.5+(1/3)b}VO_4 + {}_bLi + b\,e^-$$

The composition of the final reaction products at $x = 0.0$ is "$LiCuVO_4$."

Two cathode components, $LiCuVO_4$ and the new phase $Li_{2.5}Cu_{0.5}VO_4$, might participate in the recharge reaction from $x = 1.0$. The XRD measurements of the cathode recharged from $x = 1.0$ to 0.0, however, showed no significant difference in the lattice parameters from those of the stoichiometric spinel. This indicates that lithium ions did not deintercalate from the spinel $LiCuVO_4$ and that only the new phase participated in the reaction.

For the second discharge of the cathode charged from $x < 1.5$, two components with different mechanisms might participate in the reaction; $LiCuVO_4$ reacts with lithium by a multiphasic process, and the new phase with a composition of "$LiCuVO_4$" by a monophasic electrochemical displacement reaction. The discharge profile in the range of $0 < x < 1.5$ gradually changes up to 10 cycles, which indicates that the amount of Li $CuVO_4$ spinel decreases and the new phase increases with cycling. For the charge process, on the other hand, no change in profile is observed. Therefore, only the new phase participates in the recharge reaction. For $1.5 < x < 2.0$, the cathode composed of the new phase reacts with lithium by the monophasic electrochemical displacement

TABLE III

EXAMPLES OF THE ELECTROCHEMICAL DISPLACEMENT REACTION

Compound	Cations participate in the displacement reaction	Ref.
$AgV_2O_{5.5}$	Ag → Li	(*22*)
α-$Cu_2V_2O_7$	Cu → Li	(*23*)
$CuV_{2-x}Mo_xO_6$	Cu ↔ Li	(*24*)
$NiPS_3$	Ni → Li	(*25*)
$M_xMo_6S_8$ (Chevrel phase)	Cu ↔ Li Ag In Tl → Li Sn	(*14, 26–28*)
α-Fe_2O_3	Fe → Li	(*29*)
$LiFe_5O_8$ (Spinel)		
$LiCuVO_4$	Cu ↔ Li	This work

reaction, which leads to no significant change in the charge–discharge profiles for the cell cycled at $x = 1.9 \pm 0.05$.

The electrochemical displacement reaction. Table III summarizes the electrochemical displacement reaction for the framework structures reported previously. The lithiation proceeded by several steps in the silver vanadium bronze, which is formed by the VO_x-linked three-dimensional framework (*22*). The chemical analysis of the lithiated samples showed a decrease in vanadium valence state from V to IV, and silver was reduced to the metallic state. In the copper vanadate α-$Cu_2V_2O_7$, copper metal also extruded from the framework structure by the discharge (*23*). Recent studies on $CuV_{2-x}Mo_xO_6$ ($0 \leq x \leq 1.0$) showed reversible cell reaction by the displacement between lithium and copper ions (*24*).

The electrochemical displacement reaction is also studied in the Chevrel phase, $M_xMo_6S_8$ (*14, 26–28*). The structure of the Chevrel phase consists of a three-dimensional packing of Mo_6S_8 clusters with large empty cavities for the uptake of guest metal species. The electrochemical displacement was reported for the *M* species of Cu, Ag, In, and Tl, which were displaced electrochemically by lithium at the early few discharge–charge cycles. The lithium cell reaction was highly reversible and a part of the copper removed on discharge reentered the host on charge. The reduction process was also reported for $NiPS_3$ with a layer structure; nickel metal extruded from the structure with lithium intercalation (*25*). The electrochemical extrusion of iron reported for the spinal structure proceeded at higher temperature, since the ionic diffusion at room temperature is too slow for the reaction to proceed (*29*).

The phase $Li_{2.5}Cu_{0.5}VO_4$ obtained from the spinel $LiCuVO_4$ is an example which shows electrochemical displacement between copper and lithium ions. It is apparent from Table III that the reversible reaction is found for $CuV_{2-x}Mo_xO_6$, the Chevrel phase $Cu_xMo_6S_8$ (some copper ions reenter the structure) and $Li_{2.5}Cu_{0.5}VO_4$. The reversible displacement therefore takes place when the cations responsible for the reaction are quite mobile, such as copper and lithium ions.

Conclusion

Electrochemical and structural characterization of the spinel $LiCuVO_4$ has led to the following conclusions:

(1) The spinel $LiCuVO_4$ transforms to copper metal and the new phase, "$Li_{2.5}Cu_{0.5}VO_4$," at $x = 1.5$ in $Li_{1+x}CuVO_4$ by the first discharge with a multiphasic reaction.

(2) The spinel $LiCuVO_4$ does not participate in the charge process.

(3) The cathode with $Li_{2.5}Cu_{0.5}VO_4$ is rechargeable by the electrochemical displacement between copper and lithium ions. The reaction is quite reversible and no significant degradation of the charge–discharge properties was observed for more than 100 cycles.

References

1. M. S. WHITTINGHAM, *Prog. Solid State Chem.* **12,** 41 (1978).
2. Y. TAKEDA, R. KANNO, T. TANAKA, AND O. YAMAMOTO, *J. Electrochem. Soc.* **134,** 641 (1987).
3. Y. TAKEDA, R. KANNO, Y. TSUJI, AND O. YAMAMOTO, *J. Electrochem. Soc.* **131,** 2006 (1984).
4. K. MIZUSHIMA, P. C. JONES, P. J. WISEMAN, AND J. B. GOODENOUGH, *Mater. Res. Bull.* **15,** 783 (1980).
5. R. KANNO, Y. TAKEDA, AND O. YAMAMOTO, *Solid State Ionics* **28–30,** 1276 (1988).
6. J. B. GOODENOUGH, *in* "Physics and Chemistry of Electrons and Ions in Condensed Matter," (J. V. Acrivos, N. F. Mott, and A. D. Yoffe, Eds.), Reidel, Dordrecht (1983).
7. M. M. THACKERAY, W. I. F. DAVID, AND J. B. GOODENOUGH, *Mater. Res. Bull.* **17,** 785 (1982).
8. M. M. TACKERAY, W. I. F. DAVID, P. G. BRUCE, AND J B. GOODENOUGH, *Mater. Res. Bull.* **18,** 461 (1983).
9. R. J. CAVA, D. W. MURPHY, S. ZAHURAK, A. SANTORO, AND R. S. ROTH, *J. Solid State Chem.* **53,** 64 (1984).
10. L. A. DE PICCIOTTO AND M. M. THACKERAY, *Mater. Res. Bull.* **20,** 1409 (1985).
11. W. I. F. DAVID, M. M. THACKERAY, L. A. DE PICCIOTTO, AND J. B. GOODENOUGH, *J. Solid State Chem.* **67,** 316 (1987).
12. A. C. W. P. JAMES AND J. B. GOODENOUGH, *Solid State Ionics,***27,** 37 (1988).
13. R. KANNO, Y. TAKEDA, K. TAKADA, AND O. YAMAMOTO, *J. Electrochem. Soc.* **131,** 469 (1984).
14. Y. TAKEDA, R. KANNO, M. NODA, AND O. YAMAMOTO, *Mater. Res. Bull.* **20,** 71 (1985).
15. R. KANNO, Y. TAKEDA, M. HASEGAWA, O. YAMAMOTO, AND N. KINOMURA, to be published.
16. M. EISENBERG, *Electrochim. Acta* **26,** 955 (1981).
17. L. A. DE PICCIOTTO AND M. M. THACKERAY, *Mater. Res. Bull.* **21,** 583 (1986).
18. M. M. THACKERAY, W. I. F. DAVID, P. G. BRUCE, AND J. B. GOODENOUGH, *Mater. Res. Bull.* **18,** 461 (1983).
19. M. M. THACKERAY, P. J. JOHNSON, L. A. DE PICCIOTTO, P. G. BRUCE, AND J. B. GOODENOUGH, *Mater. Res. Bull.* **19,** 179 (1984).
20. P. SCHON, *Surf. Sci.* **35,** 96 (1973).
21. C. BLAAUW, F. LEENHOUTS, F. VAN DER WOUDE, AND G. A. SAWATZKY, *J. Phys. C.* **8,** 459 (1975).
22. E. S. TAKEUCHI AND W. C. THIEBOLT III, *J. Electrochem. Soc.* **135,** 2691 (1988).
23. Y. SAKURAI, H. OHTSUKA, AND J. YAMAKI, *J. Electrochem. Soc.* **135,** 32 (1988).
24. Y. TAKEDA, K. ITO, O. YAMAMOTO, AND R. KANNO, *J. Electrochem. Soc.*, in press.
25. R. BREC, *Solid State Ionics* **22,** 3 (1986).
26. W. R. MCKINNON AND J. R. DAHN, *Solid State Commun.* **52,** 245 (1984).
27. J. M. TARASCON, T. P. ORLANDO, AND M. J. NEAL, *J. Electrochem. Soc.* **135,** 804 (1988).
28. J. M. TARASCON, F. J. DISLVO, D. W. MURPHY, G. W. HILL, E. A. RIETMAN, AND J. V. WASZCZAK, *J. Solid State Chem.* **54,** 204 (1984).
29. M. M. THACKERAY, W. I. F. DAVID, AND J. B. GOODENOUGH, *J. Solid State Chem.* **58,** 280 (1984).